Predicting Future Tumor Location in Patients with Brain Metastases

A Technical Report submitted to the Department of Biomedical Engineering

Presented to the Faculty of the School of Engineering and Applied Science

University of Virginia • Charlottesville, Virginia

In Partial Fulfillment of the Requirements for the Degree

Bachelor of Science, School of Engineering

Connor G. Grubbs

Spring, 2020

Technical Project Team Members

Pamela Flitsch Medina

On my honor as a University Student, I have neither given nor received unauthorized aid on this assignment as defined by the Honor Guidelines for Thesis-Related Assignments

Dr. Williams Watkins, Department of Radiation Oncology

Predicting Future Tumor Location in Patients with Brain Metastases

Connor G. Grubbs[a,*]. Pamela S. Flintsch Medina[a,*], William T. Watkins[b]

[a] Biomedical Engineering, University of Virginia
[b] Department of Radiation Oncology, University of Virginia
* Authors contributed equally on this work
[1] Correspondence: cgg4xa@virginia.edu

Abstract

Brain Metastases are a serious complication for cancer patients, with incidence rates up to 40% for some primary cancers. Gamma Knife Radiosurgery (GKS) is a procedure that allows for precise targeting of radiation treatment within the brain without exposing untargeted locations to high levels of radiation. Currently, GKS treatment plans are developed by physicians based on an array of magnetic resonance imaging (MRI) including contrast-enhanced T1 images, T2 images, and in some cases diffusion and perfusion MRIs. Treatment plans are designed based on the human examination of the brain and identification of lesions. This process is susceptible to inter-observer variation, planning and targeting experience, and is limited in the ability to detect regions of new cancer growth. This work investigates novel machine learning algorithm applications to improve these processes. Specifically, we evaluate a transfer learning of image-based deep convolutional networks for the purpose of predicting brain metastases formation. The trained network demonstrated the ability to discriminate between healthy and pre-tumor tissue with up to 68% accuracy. Identified modifications and improvements may increase the predictive power of the algorithm and offer potential areas for future investigation.

Keywords: Brain Metastases, Gamma Knife Surgery (GKS), Machine Learning, MRI

Introduction

Brain metastasis is a significant consideration and complication in developing cancer treatment plans. Estimates for the percentage of cancer patients who develop brain metastasis has been reported as ranging from 20-40% depending on the type of data reviewed[1]. This range, however, likely understates the actual incidence rate. The majority of these estimates are based on sets of historical data in which metastasis may not have been accurately documented, especially in the case of discovery in terminally ill patients and asymptomatic metastasis[2]. Additionally, as identification and treatment of primary cancers continue to increase patient survival time, the incidence rates for brain metastasis also increase[3]. One of the main factors contributing to brain metastasis incidence is the histology of the primary cancer. Lung cancer is the most common primary cancer to develop brain metastasis with incidences up to 65%. Other high incidence cancers include breast cancer and melanoma[4]. Brain metastases contribute unique neurological clinical manifestations that can further decrease the quality of life of cancer patients. The most common presenting symptom for brain metastases is headaches (50%), followed by focal weakness (27%) and change in mental status (31%). Seizures are a less common presenting symptom (10%) but occur in a significant amount (40%) of patients over the course of the illness[5]. For some patients, neurological symptoms are so debilitating, that the brain metastases are identified by MRI before a primary cancer is discovered[6]. The prognosis for brain metastases is not favorable with a median survival of 3.4 months and a 2-year survival percentage of only 4%[7]. Lagerwaard et al. show that patient prognosis has a significant dependence on treatment method.

Gamma Knife Radiosurgery (GKS) has become increasingly used to target the aforementioned metastases and is performed on approximately 35,000 patients a year[8,9,10]. Gamma knife utilizes cobalt 60 to create 201 focused gamma rays which lesion the area of interest[8]. GKS is noninvasive and has been found to have an accuracy within than 3mm when focused on a single-isocenter[11,12].

Treatment can be delivered within a single session with limited patient exposure to radiation, and complications from the treatment are uncommon[13,14]. These factors along with the treatments greater than 90% success rate for controlling tumor growth contribute to its large appeal as a treatment option[8,14]. GKS is an especially effective tool for the treatment of brain metastasis[10] in which multiple recurring tumors are common. Clinically treatment plans are constructed using guidelines set forth by the Radiation Therapy Oncology group corresponding to conformation index and target coverage[15]. Conformation index is an indicator of how well the dose conforms to the shape of the tumor, while target coverage allows us to analyze the portion of the tumor covered by the dosage. Existing protocol states treatment plans should achieve a minimum of 80% target coverage and a conformity index of .8, with ideal values being above 95% and .9 respectively[16].

Many applications of machine learning in the medical field are being heavily explored and show promising results. Within radiology, machine learning has been used to optimize assessment of tumor treatment areas and dosage calculations to prevent unnecessary patient exposure to radiation[17]. Machine learning has also been implemented in the automation of differentiation between benign and malignant breast cancer tumors using MRI data[18]. The model was able to differentiate with a sensitivity of 99.5% and recommended 9.6% fewer biopsies, indicating implementation would improve patient care. Additionally, machine learning has proved a useful tool in the study of proteomics, genomics, and drug delivery[19,20,21]. Due to its prevalence and utility in the medical field, a machine learning approach was used in order to determine areas of interest to monitor for future tumor formation.

Results

Creating a Tumor Dataset

Tumor Capturing Pipeline

A pipeline was created that collects uniform images of locations in all the patient MR images that at some timepoint, throughout the time of care, contained a tumor. Figure 1 shows a graphical workflow of the pipeline. IN the first step, patient data is separated by its treatment index and labeled sequentially. The dataset consisted of 15 patients of which nine had two treatments, three had three treatments, two had four treatments, and one had five treatments. In total the study consisted of 40 individual treatments. Within each treatment, the MRI positioning and size was standardized such that a specific pixel coordinate set corresponds to the same brain geometry across all treatments for a patient. To facilitate this, every treatment MRI was registered to a 1x1x1 mm reference MR.

After the registration of the individual treatment MR images to the reference MR, the individual tumors present at the time of treatment were also registered to the reference MR. The registration of the tumors was carried out using a binary masking method based off the doses applied during the GKS treatment.

With the registration of the treatment MR and all the tumors onto the reference complete, a uniformly sized 2D square image was captured at the tumor centroid for each tumor across all treatment reference MR images within each patient set. This allowed for the capture of brain tissue areas from treatment 1 MR images that were later shown to include tumors in treatment 2. Using this methodology, the pipeline identified areas of pretumor tissue, and developed a data set that would be used to train the network.

Quality Control

Tumor images underwent manual quality control by the team to check for two known cases that may corrupt the tumor image data. The first error occurred when the treatment MR images were not properly registered to the reference MR. This error resulted in images with obvious blurring or shifted brain geometry. Additionally, in some cases tumors were identified but deemed by the treatment planner no to undergo GKS at that particular time-point. In these cases, identifiable tumors are included in the dataset as unidentified pretumor areas. To mitigate the effect of these areas, both these sets of images were removed when they were discovered.

Creating a Healthy Dataset

The healthy image dataset was created utilizing the reference MR after the treatment MR and tumors were registered. The reference MR for each treatment within a single patient was overlaid representing every tumor the patient developed across all treatments. Uniformly sized 2D square healthy images were pulled from the area of the brain across all treatments which had no registered tumors.

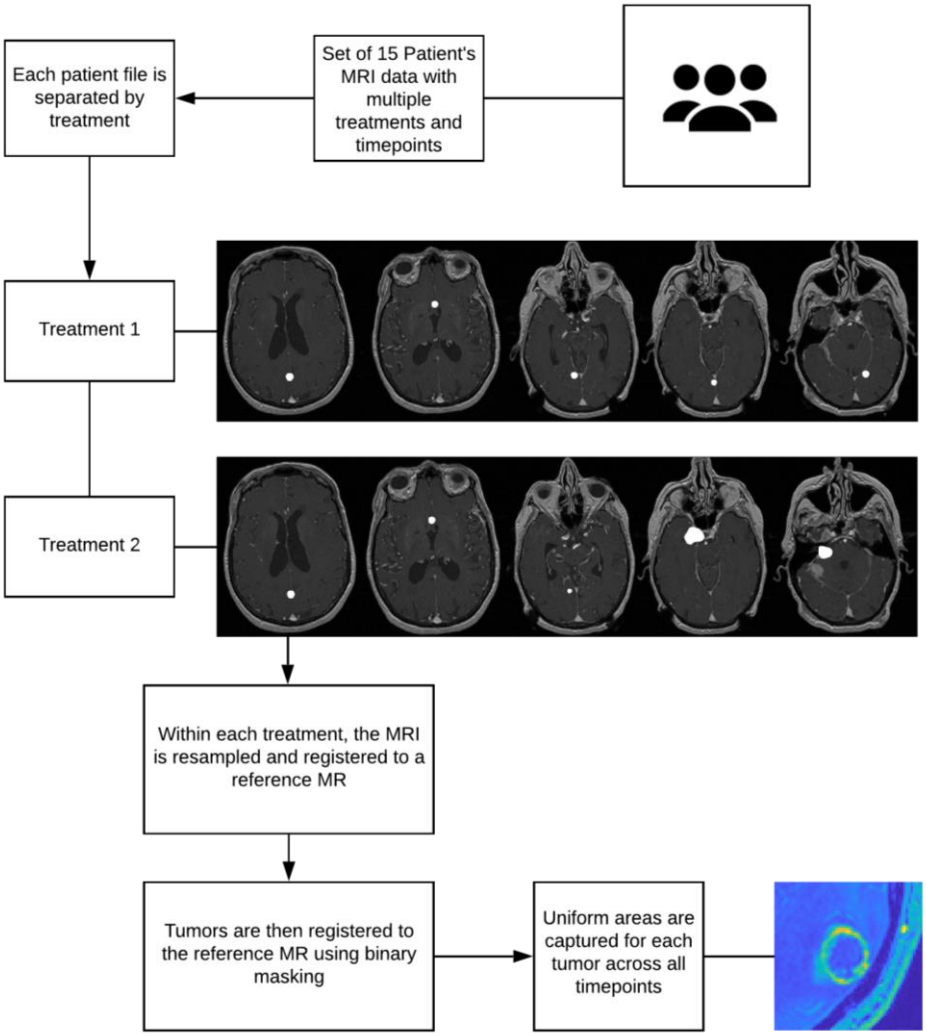

Fig. 1. Workflow for Tumor Training data Pipeline. Workflow shows the steps in processing the raw MRI data into uniform images of tumor tissue for the training dataset.

Preparing Images for Classification

Before ingestion into the classification network the patient MR images need to move through a processing pipeline (Figure 2). First, 3D volumes are separated into 2D horizontal slices, the same orientation used for the training dataset.

After the MRI is separated into individual slices, the brain tissue is isolated using a segmentation algorithm we developed. This algorithm works through a series of image processing operations to form a binary map of the brain tissue region, excluding surrounding air and skull data.

After segmentation, a sliding window algorithm was designed to capture uniform images of the brain similar to those captured for the training dataset. These individual images are entered into the network for classification.

Designing a Classification Network

A supervised transfer learning approach was utilized to create our classification algorithm. The existing network that was adapted for this work was AlexNet[22]. AlexNet was chosen because it has shown to be a successful architecture for classification in brain MRI studies[23,24]. The final two layers of the network architecture were replaced such that the network outputs a binary classification, “tumor” or “healthy.” A random 90/10% jackknife method was used to designate training and testing data.

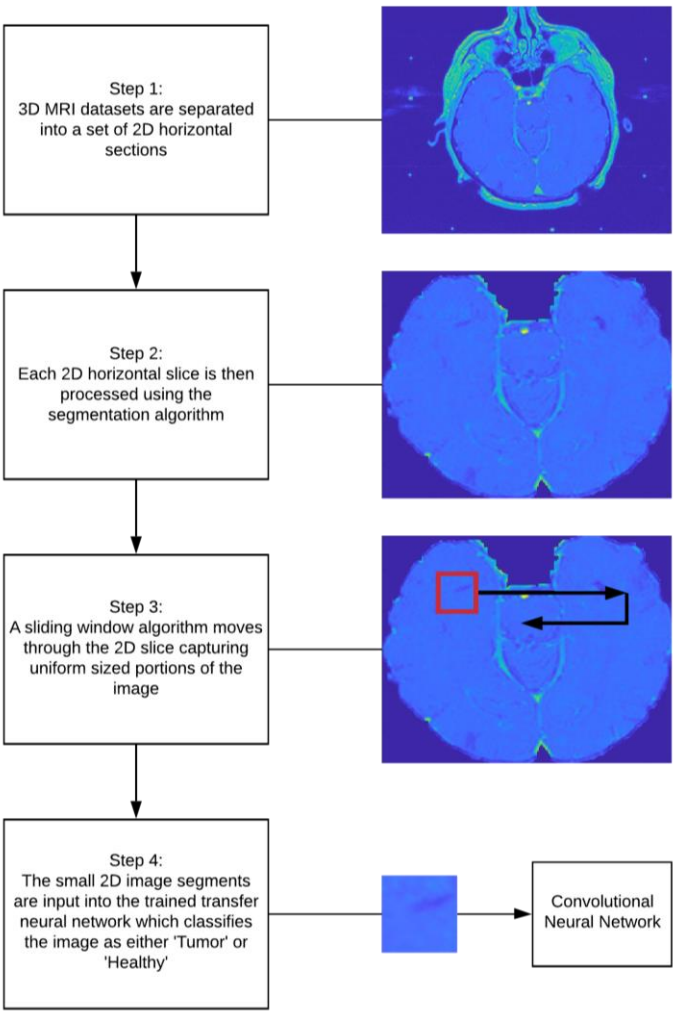

Fig. 2. Workflow of the Classification Algorithm. Workflow shows the steps in the classification algorithm. Major steps include 2D separation, brain segmentation, uniform image capture, and injection into the neural network. The convolutional neural network uses the AlexNet architecture.

Classifier Performance

Over a set of 20 training runs, the accuracy of the classifier ranged from 58-68% with an average of 64%. For these tests, the network was tested with equal amounts of "tumor" and "healthy" data such that an accuracy of 50% would indicate zero predictive power, similar to flipping a coin. The output from one of these trainings is displayed in figure 3. In the figure, the blue line indicates the accuracy of the training data over the duration of training while the black dots indicate the validation accuracy over the duration of the training. The validation data is randomly pulled from training dataset every three training cycles, representing how the algorithm would perform on the whole set of data at any given time. The variation in accuracy comes from the random jackknife of training and testing data. With a relatively small sample of tumor and healthy images, the random variation in the images selected to train the network can cause considerable differences in the final accuracy. The difference between the training and validation curves represent overfitting. Overfitting occurs when the network is identifying distinguishable features of the training images that do not hold true for the validation, or testing, data. This overfitting may also be a function of the limited dataset and the variation created by randomly selecting training data from it.

Discussion

Implications and Significance

The innovation behind the algorithm design is driven by the assertion that early identification expands treatment options, thereby potentially increasing long term survivability and standard of living. There is a large body of prior research attempting to predict brain metastases incidence based on genomic, clinical, and biological markers[25]. The major difference in the aim of these papers compared to this approach is incidence versus location. Specifically, this study sought to identify where future brain metastases will grow based on the image data from MRI, regardless of whether or not prior metastatic brain tumors have been identified. Additionally, since the approach is purely based on image information, it is independent of the histology of the primary cancer, which is unknown in some patients. This capability would be very beneficial for patients who have multiple recurrent brain metastases and are currently required to undergo consistent MRI appointments followed by GKS. Identifying, and potentially treating, cancerous locations in the brain before a tumor is visually present may increase patient survivability, as well as save patient and hospital resources. Additionally, for patients with primary cancers associated with high incident rates of brain metastases, such as lung and breast cancer[26], this capability may prove especially useful. In this instance the algorithm could be used as a preventative tool to identify pretumor locations. This would allow physicians to locate tumors prior to the presentation of the associated neurological symptoms that can significantly decrease quality of life. While the results did not represent especially high predictive power, they do represent evidence that machine learning approaches may be able to detect brain metastases formation from imaging data before the tumors are discernable to the trained eye.

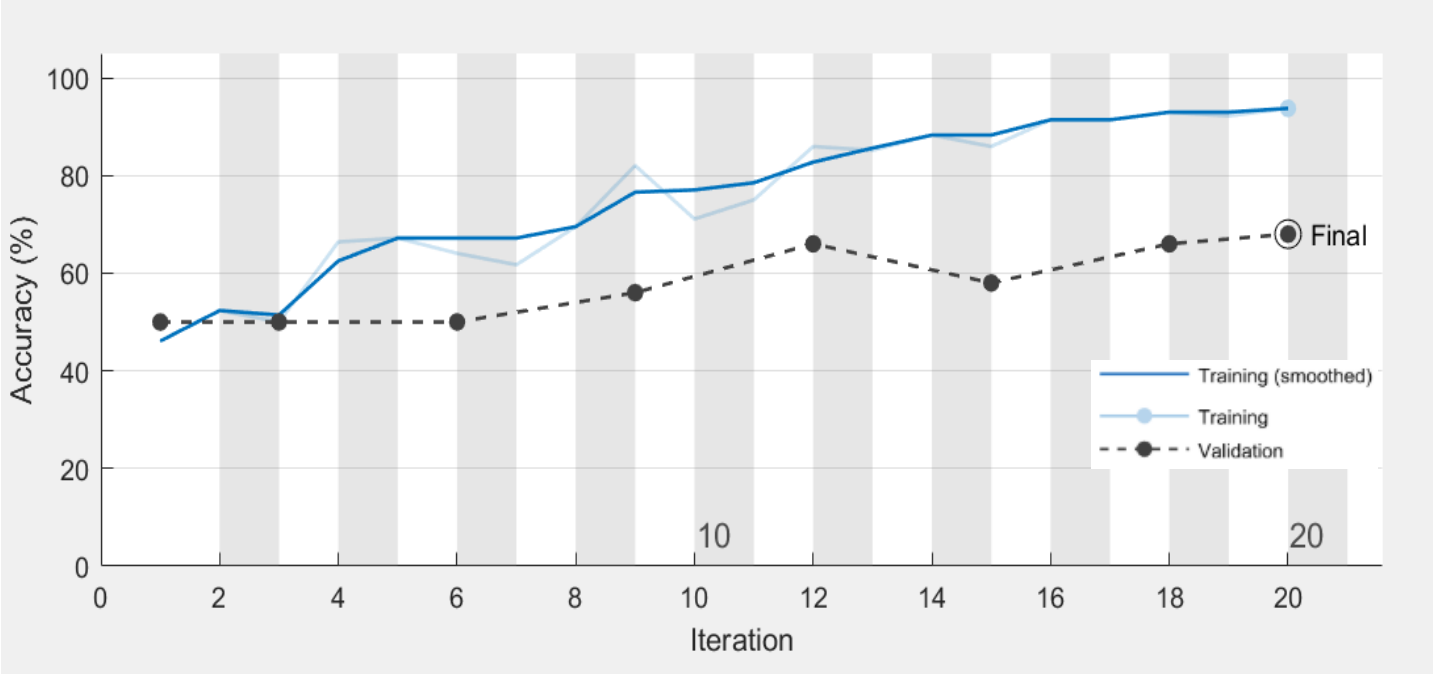

Fig. 3. Example of Convolutional Neural Network Training Progress. This is representative of the shape of all the training iterations completed in MATLAB. The dark blue line is a smoothed curve showing the accuracy of the training data. The black dots are the validation accuracy which occurred every third iteration.

Further work

There are multiple potential avenues for future investigation stemming from the work presented in this paper. A portion of the opportunities for future work arise from sources of error in our methodology. First, a new source could be identified for the "healthy" training data. In this study, healthy tissue was extracted from the patient dataset and defined as any area in which no tumors were observed across any treatment for that particular patient. This method is inherently flawed because the hypothesis assumes that tumors are constantly forming in the brain, so even though there was no tumor in a specific location at the time that patient care ended, this does not mean that a tumor was not going to form there in the future. Due to this, further investigation that uses a separate and unique source for T1-weighted MRI data may provide better results. Potential sources that we looked into include MRI data captured for use in cognition and psychology studies which evaluated test subjects with no known brain pathology. Additionally, further improvement of the algorithm could be achieved through quality control of the treatment MR and tumor registration algorithm. As described in the results, there were multiple incidences of poor registration that required manual correction. This manual correction had downstream ramifications in that this area was now not being counted as "tumor" and was potentially being captured in "healthy" images.

Further work was also identified that could expand upon the findings. Primarily, acquiring a significantly larger set of training data would likely provide more consistency to the results. Using larger datasets, in which a single image of small set of images will not significantly skew the learning of the network, may result in less variation in the accuracy and less overfitting. Another potential expansion on the work would be implementing the methods described with other CNN architectures. AlexNet is a popular choice within diagnostic imaging, but other architectures may provide advantages in accuracy for this problem set. Finally, evaluating the impact of edge images on the network may prove useful in increasing the accuracy of the algorithm. These images capture the edge of the brain tissue and inherently some of the empty space around the brain. This is a result of the removal of the skull and air data that occurs in the image processing segmentation algorithm. With deep learning networks it is difficult to pinpoint what features about the images the network is using to guide its learning, and we want to minimize the potential for features not relevant to our question to influence the classifier.

Materials and Methods

Patient MRI Collection

Patient MRI data was collected from 15 patients who were treated at the University of Virginia Gamma Knife Center. All MR images used in this design were T1-weighted images. A single patient set was used as a validation set while designing the registration, segmentation, and network algorithms. This dataset was appropriately stripped of all identifying information and included randomized noise to anonymize the image data. The full set of MRI data used for training and testing were anonymized using a naming system developed by the team that referenced the patient number (1-15), the treatment number, and the tumor number. With consultation from the IRB the final dataset has been deemed a "Limited Dataset," which does not require HIPAA authorization or waiver and is intended only for research purposes.

Registration of MR to Reference

Every MR image was registered to a reference MR in MATLAB. First, a three-component registration scaling factor (*rs*) was calculated, according to equation 1, in which mr_x, mr_y, and mr_z correspond to the size of the MR

$$rs = \left[\frac{1}{mr_x}, \frac{1}{mr_y}, \frac{1}{mr_z}\right] \quad [1]$$

image in each dimension. The numerator 1 comes from the size of the reference MR which is 1 mm x 1 mm x 1mm. This was then used to resize the 3D volume according to the dimension specific value. A one plus one evolutionary optimizer was then calculated for the registration operation. The algorithm works by iterating through a set of perturbations to find an optimized set of registration parameters[27]. A Mattes mutual information algorithm was then used to find the configuration metric for the image registration. The Mattes algorithm uses a single set of pixel locations to compute probability estimates and uncertainty, or entropy, of similarity between two images[28]. Next, a geometric transformation was estimated for the registration using the calculated optimizer and configuration metric. The geometric transformation is an object that maps the MR to the reference MR. Finally, an inverse mapping algorithm was used to complete the registration of the MR onto the reference MR using the geometric transformation object.

Registration of Tumors to Reference

For each MR, the tumor dosages were registered to a reference MR in MATLAB. First, a three-component registration scaling factor (*rs*) was calculated according to equation 1. Next, a dose mask was created by extracting the volume dimensions for each of the resized tumors. A one plus one evolutionary optimizer was then calculated for the registration operation. The algorithm works by iterating through a set of perturbations to find an optimized set of registration parameters[27]. A Mattes mutual information algorithm was then used to find the configuration metric for the image registration. The Mattes algorithm uses a single set of pixel locations to compute probability estimates and uncertainty, or entropy, of similarity between two images[28]. Next, a geometric transformation was estimated for the registration using the calculated optimizer and configuration metric. The geometric transformation is an object that maps the dose mask to the reference MR. Finally, an inverse mapping algorithm was used to complete the registration of the dose mask onto the reference MR using the geometric transformation object.

Collecting Tumor Images

Compilation of the tumor image data was completed in MATLAB. After all the tumors for a single patient were registered onto the reference MR, the area around the tumor was captured for all previous time points. The tumor dataset contained 127 images.

Collecting Healthy Images

Compilation of the healthy image data was completed in MATLAB. After all the tumors for a single patient were registered onto the reference, the sets of continuous area without a tumor were selected as healthy regions. Within these regions, every complete square image that was possible within the healthy region was captured. The healthy dataset contained 467 images.

Segmentation Algorithm

Normalization

MR images were normalized in MATLAB. All pixel values were scaled from 0 to 1, such that any value greater than the average of the top 80% of pixel values was equal to 1. This method was chosen to limit the influence of extremely high pixel values on normalization.

Thresholding

MR images underwent thresholding in MATLAB to target the unwanted air and bone. Intensity values for air and bone were experimentally chosen to be values below 0.15 and above 0.42, respectively. Any pixels in either of these ranges were set to 0. Pixels between 0.15 and 0.42 were all set to 100.

Binary Erosion

MR images were eroded in MATLAB to disconnect the brain tissue from the surrounding bone. Binary erosion is a set operation where an image *A* is eroded by *B*, denoted $A \ominus B$, in a location z according to equation 2.

$$A \theta B = \{z | B_z \subseteq A\} \quad [2]$$

The erosion factor *B*, is an unweighted 10-by-10 square matrix.

Region Isolation

Region isolation was performed on eroded MR images in MATLAB. First, all image pixels were scanned and labels were assigned to nonzero pixels and recorded in a union-find matrix. Then equivalence classes were resolved using the union-find algorithm[29]. This algorithm treats the union-

find matrix like a graph and finds all the sets of nodes with continuous edges. Finally, all pixels were relabeled based on their resolved equivalence classes. The pixel locations for the largest continuous area set, presumed to be brain tissue, were set to 1, while all other pixels were set to 0. The resulting matrix was a binary map of the isolated eroded brain tissue.

Binary Dilation

The brain tissue binary map was dilated in MATLAB to recover the edges that were lost in the erosion process. Binary dilation of *A* by *B* is denoted $A \oplus B$ according to equation 3, in which $\hat{B}$ is the reflection of the

$$A \oplus B = \left\{ z | \left(\hat{B}\right)_z \cap A \neq \emptyset \right\} \quad [3]$$

structuring element *B*, and *z* is the set of pixel locations. The dilation factor *B*, is an unweighted 10-by-10 square matrix.

Image Fill

The brain tissue binary map was filled to recover any internal information loss in MATLAB. Image filling was completed using a morphological reconstruction algorithm[30].

Convolutional Neural Network

Convolutional neural network (CNN) design, training, and testing was completed in MATLAB. The set of 'Tumor' and 'Healthy' images were each split into training and testing sets using a random 90/10 jackknife method. The transfer learning approach utilized the architecture from AlexNet[22]. All images were resized to the necessary 227x227 pixel input size for AlexNet, since the images were already square, no proportionality was disrupted. The final fully connected layer and classification layers were manually replaced for binary classification. The training was done over 20 epochs with validation from the testing set data

Solver Optimizers

Three separate optimizers were tested to maximize the performance of the algorithm: stochastic gradient descent (SGD), is root mean square propagation (RMSProp), and adaptive moment estimation (Adam). For all three optimizers, an initial learning rate of 0.001 was used.

Stochastic Gradient Descent

SGD updates network parameters by taking small steps in the direction of the negative gradient of loss according to equation 4, where *l* is the

$$\theta_{l+1} = \theta_l - a\nabla E(\theta_l) \quad [4]$$

iteration number α is the learning rate, θ is the parameter vector, and E(θ) is the loss function.

Root Mean Square Propagation

RMSProp differs from SGD in that it allows learning rates that vary by parameter according to equation 5. In the equation, β_2 is the decay rate of

$$v_l = \beta_2 v_{l-1} + (1-\beta_2)[\nabla E(\theta_l)]^2 \quad [5]$$

the added moving average.

Adaptive Moment Estimation

Adam is similar to RMSProp but adds a momentum term according to equation 6. In the equation, β_1 is a separate decay rate specific to the

$$m_l = \beta_1 m_{l-1} + (1-\beta_1)\nabla E(\theta_l) \quad [6]$$

new momentum term.

End Matter

Author Contributions and Notes

C.G.G, P.S.F.M, and W.T.W designed research, C.G.G, P.S.F.M, and W.T.W performed research, C.G.G, P.S.F.M, and W.T.W wrote algorithm, C.G.G and P.S.F.M. analyzed data; and C.G.G and P.S.F.M. wrote the paper.
The authors declare no conflict of interest.

Acknowledgments

We would like to thank Dr. Timothy Allen and Dr. Shannon Barker for their advisement.

References

1. Nussbaum ES, Djalilian HR, Cho KH, Hall WA. Brain metastases: Histology, multiplicity, surgery, and survival. Cancer. 1996;78(8):1781–8.
2. Gavrilovic IT, Posner JB. Brain metastases: epidemiology and pathophysiology. J Neurooncol. 2005 Oct 1;75(1):5–14.
3. Fox BD, Cheung VJ, Patel AJ, Suki D, Rao G. Epidemiology of Metastatic Brain Tumors. Neurosurg Clin. 2011 Jan 1;22(1):1–6.
4. Nayak L, Lee EQ, Wen PY. Epidemiology of brain metastases. Curr Oncol Rep. 2012 Feb;14(1):48–54.
5. Klos KJ, O'Neill BP. Brain Metastases. The Neurologist. 2004 Jan;10(1):31.
6. Brain metastases from an unknown primary tumour: which diagnostic procedures are indicated? | Journal of Neurology, Neurosurgery & Psychiatry [Internet]. [cited 2019 Oct 25]. Available from: https://jnnp.bmj.com/content/61/3/321.short
7. Lagerwaard F, Levendag P, Nowak PeterJCM, Eijkenboom WilhelminaMH, Hanssens PatrickEJ, Schmitz PaulIM. Identification of prognostic factors in patients with brain metastases: a review of 1292 patients. Int J Radiat Oncol. 1999 Mar 1;43(4):795–803.
8. Lindquist. Gamma Knife Radiosurgery. Semin Radiat Oncol. 1995 Jul;5(3):197–202.
9. History and Technical Overview [Internet]. Neurosurgery. [cited 2019 Oct 25]. Available from: https://med.virginia.edu/neurosurgery/services/gamma-knife/for-physicians/history-and-technical-overview/
10. Petrovich Z, Yu C, Giannotta SL, O'day S, Apuzzo MLJ. Survival and pattern of failure in brain metastasis treated with stereotactic gamma knife radiosurgery. J Neurosurg. 2002 Dec 1;97(Supplement 5):499–506.
11. Ma L, Chuang C, Descovich M, Petti P, Smith V, Verhey L. Whole-procedure clinical accuracy of gamma knife treatments of large lesions. Med Phys. 2008 Nov;35(11):5110–4.

12. Lunsford LD, Flickinger J, Lindner G, Maitz A. Stereotactic Radiosurgery of the Brain Using the First United States 201 Cobalt-60 Source Gamma Knife. Neurosurgery. 1989 Feb 1;24(2):151–9.

13. Comparison Gamma Knife to CyberKnife [Internet]. Neurosurgery. [cited 2019 Oct 25]. Available from: https://med.virginia.edu/neurosurgery/services/gamma-knife/for-physicians/comparison-gamma-knife-to-cyberknife/

14. Chin LS, Lazio BE, Biggins T, Amin P. Acute complications following gamma knife radiosurgery are rare. Surg Neurol. 2000 May;53(5):498–502; discussion 502.

15. Shaw E, Kline R, Gillin M, Souhami L, Hirschfeld A, Dinapoli R, et al. Radiation therapy oncology group: Radiosurgery quality assurance guidelines. Int J Radiat Oncol. 1993 Dec 1;27(5):1231–9.

16. Lomax NJ, Scheib SG. Quantifying the degree of conformity in radiosurgery treatment planning. Int J Radiat Oncol. 2003 Apr 1;55(5):1409–19.

17. Garcia-Sanchez A-J, Garcia Angosto E, Llor JL, Serna Berna A, Ramos D. Machine Learning Techniques Applied to Dose Prediction in Computed Tomography Tests. Sensors [Internet]. 2019 Nov 22 [cited 2020 Jan 31];19(23). Available from: https://www.ncbi.nlm.nih.gov/pmc/articles/PMC6928694/

18. Ji Y, Li H, Edwards AV, Papaioannou J, Ma W, Liu P, et al. Independent validation of machine learning in diagnosing breast Cancer on magnetic resonance imaging within a single institution. Cancer Imaging [Internet]. 2019 Sep 18 [cited 2019 Oct 1];19. Available from: https://www.ncbi.nlm.nih.gov/pmc/articles/PMC6751793/

19. Fox T, Kriegl JM. Machine Learning Techniques for In Silico Modeling of Drug Metabolism [Internet]. 2006 [cited 2020 Jan 31]. Available from: https://www.ingentaconnect.com/content/ben/ctmc/2006/00000006/00000015/art00003

20. Leung MKK, Delong A, Alipanahi B, Frey BJ. Machine Learning in Genomic Medicine: A Review of Computational Problems and Data Sets. Proc IEEE. 2016 Jan;104(1):176–97.

21. Sonsare PM, Gunavathi C. Investigation of machine learning techniques on proteomics: A comprehensive survey. Prog Biophys Mol Biol. 2019 Sep;S0079610719301385.

22. Krizhevsky, A., Sutskever, I., Hinton, G.E., ImageNet Classification with Deep Convolutional Neural Networks. Advances in Neural Information Processing Systems. 2012.

23. Lu, S., Lu, Z., Zhang, YD. Pathological brain detection based on AlexNet and transfer learning. J of Comp Sci. 2019 Jan; 30:41-47

24. Khagi, B., Lee, CG, Kwon, GR. Alzheimer's disease classification from brain MRI based on transfer learning from CNN. Biomedical Engineering International Conference. IEEE. 2018.

25. Teplyuk NM, Mollenhauer B, Gabriely G, Giese A, Kim E, Smolsky M, et al. MicroRNAs in cerebrospinal fluid identify glioblastoma and metastatic brain cancers and reflect disease activity. Neuro-Oncol. 2012 Jun 1;14(6):689–700.

26. Nayak L, Lee EQ, Wen PY. Epidemiology of brain metastases. Curr Oncol Rep. 2012 Feb;14(1):48–54.

27. Styner, M., C. Brechbuehler, G. Székely, and G. Gerig. "Parametric estimate of intensity inhomogeneities applied to MRI." IEEE Transactions on Medical Imaging. Vol. 19, Number 3, 2000, pp. 153-165.

28. D. Mattes, D.R. Haynor, H. Vesselle, T. Lewellen, and W. Eubank. "Non-rigid multimodality image registration." (Proceedings paper).Medical Imaging 2001: Image Processing. SPIE Publications, 3 July 2001. pp. 1609–1620.

29. Sedgewick, Robert, Algorithms in C, 3rd Ed., Addison-Wesley, 1998, pp. 11-20.

30. Soille, P., Morphological Image Analysis: Principles and Applications, Springer-Verlag, 1999, pp. 173–174.